Characterization of a cold cathode Penning ion source for the implantation of noble gases beneath 2D monolayers on metals: Ions and neutrals

Cun, Huanyao ; Spescha, Annina ; Schuler, Adrian ; Hengsberger, Matthias ; Osterwalder, Jürg ; Greber, Thomas

Abstract: Argon ion kinetic energy spectra at different discharge voltages (between 480 and 600 V) of a commercial cold cathode ion source IQP10/63 are reported. The high kinetic energy cut-off depends on the discharge voltage and the corresponding plasma potential due to excess positive charges which is found to be about 136 V. Exposure of single layer hexagonal boron nitride on rhodium to the beam of the ion source leads to the formation of nanotents, i.e., stable atomic protrusions. A positive bias voltage is applied to the target sample to block the positive ions produced by the ion source. However, application of a positive bias potential (800 eV), which is higher than the kinetic energy cut-off, still allows the formation of nanotents and its observation with scanning tunneling microscopy. This indicates that the ion source also produces neutral atoms with kinetic energies higher than the penetration threshold across a single layer of hexagonal boron nitride.

DOI: https://doi.org/10.1116/1.4939507

Characterization of a cold cathode Penning ion source for the implantation of noble gases beneath 2D monolayers on metals: Ions and neutrals

Huanyao Cun, Annina Spescha, Adrian Schuler, Matthias Hengsberger, Jürg Osterwalder, and Thomas Greber

Citation: J. Vac. Sci. Technol. A **34**, 020602 (2016); doi: 10.1116/1.4939507
View online: http://dx.doi.org/10.1116/1.4939507
View Table of Contents: http://avs.scitation.org/toc/jva/34/2
Published by the American Vacuum Society

Characterization of a cold cathode Penning ion source for the implantation of noble gases beneath 2D monolayers on metals: Ions and neutrals

Huanyao Cun,[a] Annina Spescha, Adrian Schuler, Matthias Hengsberger, Jürg Osterwalder, and Thomas Greber[a]
Physik-Institut, Universität Zürich, Winterthurerstrasse 190, CH-8057 Zürich, Switzerland

(Received 2 November 2015; accepted 21 December 2015; published 8 January 2016)

Argon ion kinetic energy spectra at different discharge voltages (between 480 and 600 V) of a commercial cold cathode ion source IQP10/63 are reported. The high kinetic energy cut-off depends on the discharge voltage and the corresponding plasma potential due to excess positive charges which is found to be about 136 V. Exposure of single layer hexagonal boron nitride on rhodium to the beam of the ion source leads to the formation of nanotents, i.e., stable atomic protrusions. A positive bias voltage is applied to the target sample to block the positive ions produced by the ion source. However, application of a positive bias potential (800 eV), which is higher than the kinetic energy cut-off, still allows the formation of nanotents and its observation with scanning tunneling microscopy. This indicates that the ion source also produces neutral atoms with kinetic energies higher than the penetration threshold across a single layer of hexagonal boron nitride. © *2016 American Vacuum Society*. [http://dx.doi.org/10.1116/1.4939507]

I. INTRODUCTION

Ion beams are well-known tools for shaping materials. Focused ion beams, a standard equipment in nanoscience laboratories,[1] operate with kiloelectron-volt energy ions for atom-milling purposes. Lower energy ion beams are used for surface characterization,[2] sputtering, and cleaning. Below the sputtering threshold, the formation of adatom and vacancy islands is observed.[3] Recently, near threshold ion scattering was applied for the shaping of atomically thin two dimensional materials such as hexagonal boron nitride (*h*-BN),[4] graphene,[5–7] or transition metal dichalcogenides,[8] and it was realized that monolayer systems on transition metals bear unique opportunities to produce nonrandom defects, if ion energies near the penetration threshold are employed.[4]

For the case of a single layer of *h*-BN on rhodium (the *h*-BN nanomesh),[9,10] it was found that atomic agglomerates may be formed in a controlled fashion.[4] The so-called "nanotents"[11] are atomic structures that are stabilized and protected by a single layer of boron nitride[4,11] or graphene[7] that acts as the "rainfly." In order to further improve the selectivity of this low ion energy implantation process, it is of ultimate importance to know the energy distribution of the ions.

Here, we report on energy spectra of a Penning type cold cathode ion source used for the formation of nanotents[4,11] and nanovoids.[7,12] Nanovoids represent another peculiar type of structure that may be formed on the *h*-BN/Rh(111) system after low energy ion exposure and subsequent annealing. It turns out that the vacancy defects due to the penetration of Ar^+ ions across the single layer of *h*-BN lead to the cut-out of 2 nm flakes from the *h*-BN nanomesh pore sites.[4,12] The present investigations reveal that the commercial Penning type cold cathode ion source IQP10/63 (Specs, Berlin) also produces neutral atoms with a kinetic energy higher than the nanotent creation threshold.

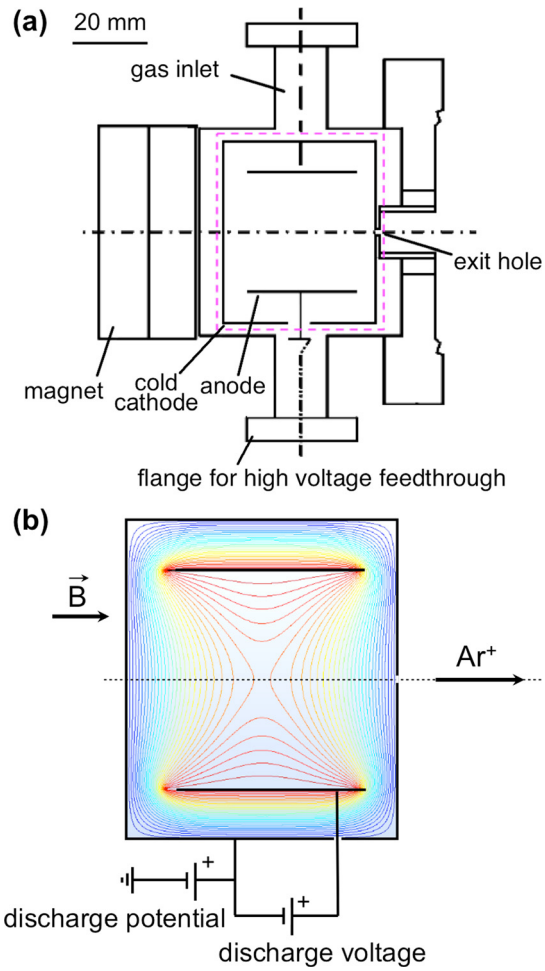

FIG. 1. (Color online) Penning ion source with cylindrical symmetry. (a) Cross section of an IQP10/63 (Specs, Berlin). (b) Vacuum electrostatic potential simulation of the plasma vessel, indicated with a pink rectangle in (a). The equipotential-lines are equidistant and indicate the ion focusing on the exit hole of the plasma vessel. The magnetic field is parallel to the gun axis and increases the ionization yield of the Ar atoms.

[a]Authors to whom correspondence should be addressed; electronic addresses: hycun1@physik.uzh.ch; greber@physik.uzh.ch

II. EXPERIMENT

The ion energy spectra of a commercial cold cathode Penning ion source IQP10/63 (Specs, Berlin) were measured in a setup where the ion beam was directed across a circular aperture into an electrostatic VG Alpha 110 electron analyzer with the lens entrance of which is 46.8 cm away from the exit of the ion gun. The polarity of the analyzer was switched to the positive ion scattering spectroscopy mode. For the measurements of the kinetic energy spectra, all lens-potentials of the analyzer were connected to ground potential. The scanning tunneling microscopy (STM) experiments were performed on an Omicron variable temperature scanning tunneling microscope.[4] In the STM experiments, the exit of the ion gun is 19 cm away from the sample and the ions for the nanotents formation impinge at an angle of 55° from the sample normal. The nanomesh sample has been biased with positive voltage in order to study the influence of the ion energy on shape and yield of nanotents during ion irradiation.

III. ION SOURCE

Cold cathode Penning type ion sources[13] are known to be efficient sputter guns for cleaning surfaces in ultrahigh vacuum. Surprisingly, however, only a few reports on the ion energy distribution curves are available.[14,15] In the following, we report the ion energy spectra for a commercial cold cathode Penning type ion source operating with argon gas.

Figure 1(a) shows a schematic drawing of the Penning ion source IQP 10/63. It has cylindrical symmetry and consists of an outer vessel, the cold cathode and an inner coaxial tube (the anode). An axial magnetic field in the order of about 75 mT is supplied by a permanent magnet and increases the electron paths, and thus the ionization probability of the gas. The ions are accelerated toward the cathode, where the specific geometry focuses a large portion onto the exit hole, from where they may escape into vacuum, and, if desired, they may be further accelerated by a discharge potential. The typical gas pressure in the vessel may be estimated from the pressure in the recipient, the pumping speed

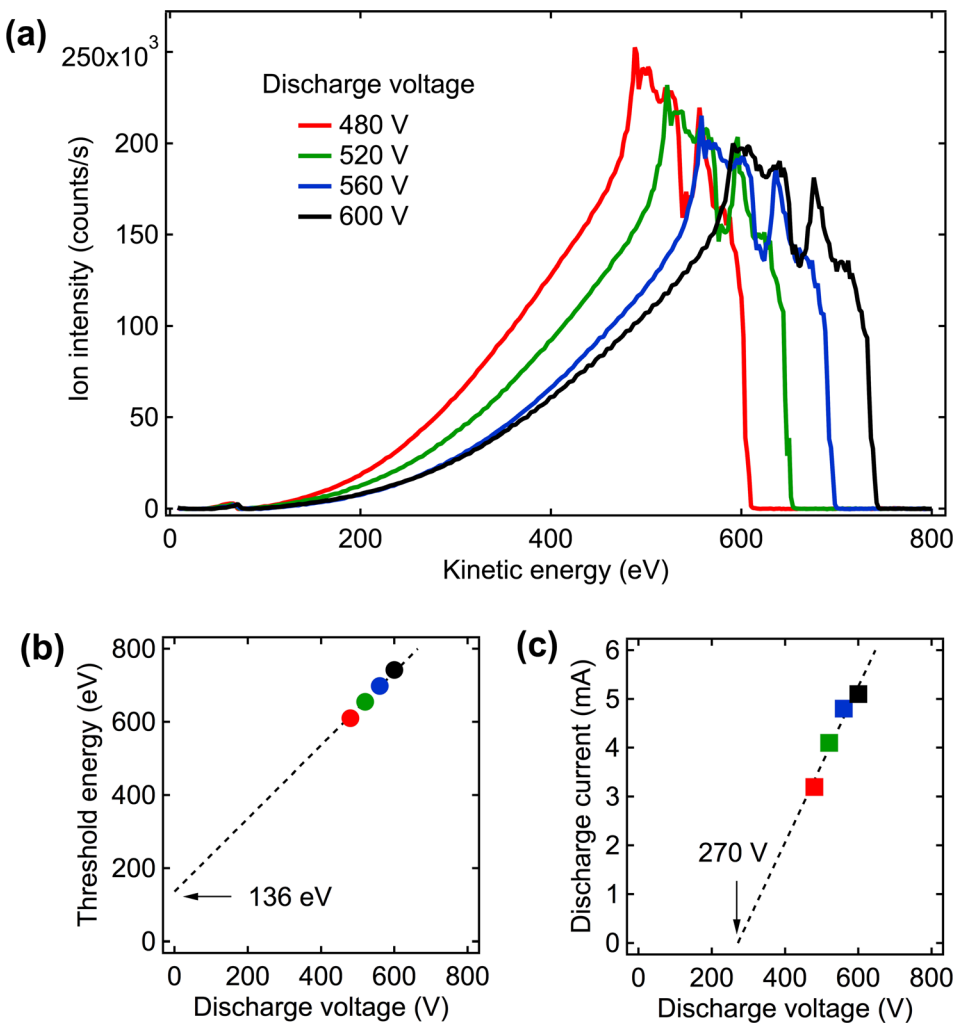

FIG. 2. (Color online) Performance of the IQP10/63 for a given Ar pressure of about 6×10^{-2} mbar in the plasma vessel. (a) Ar ion energy spectra for different discharge voltages and zero discharge potential. (b) Threshold energy vs discharge voltage. The linear extrapolation of the four measured spectra indicates a plasma potential of 136 eV that has to be added to the discharge voltage if the threshold energy shall be determined. (c) Discharge current vs discharge voltage. The linear extrapolation of the four measured discharge voltage/current pairs indicates a zero current plasma discharge voltage of 270 V and a plasma conductivity of 16 μS.

and the aperture size of the exit hole. For operation we applied a pressure of argon in the vessel of 6×10^{-2} mbar. This indicates that the mean free path of the gas is in the order of the size of the vessel (3 cm) and the maximum ion energy must be given by the discharge voltage, the plasma potential, the discharge potential, and the charge state of the ions.

From the saddle shape of the potential inside the vessel, it may furthermore be expected that the energy distribution of the ions will be broad and have an upper cut-off due to the discharge voltage, the plasma potential, and the discharge potential (see Fig. 1). The plasma potential arises due to the fact that the plasma is not charge neutral. Since the electrons are more mobile, the resulting space charge is positive and will further increase the energy of the ions leaving the vessel.

Figure 2(a) shows ion energy spectra as recorded in a setup with the ions impinging parallel to the detector axis for four different discharge voltages and zero discharge potential. As expected, the spectra are broad, though they also display sharp features. In particular, they have a threshold or maximum kinetic energy that depends on the discharge voltage. Figure 2(b) shows the four thresholds as a function of the discharge voltage.

The fit to the four discharge voltages between 480 and 600 V, where the plasma in the ion gun burns stably, is a linear function with a slope set to one electron charge. This assumes a constant plasma potential for these four discharge voltages, and the zero discharge voltage offset indicates a plasma potential of 136 eV. If the slope in the linear function is left as a free parameter, we get 1.09 ± 0.01 electron charges, which indicates that the plasma potential weakly depends on the discharge voltage. The plasma potential corresponds with the given geometry of the plasma vessel to an ion excess concentration of about 3×10^8 excess ions cm^{-3}. This estimate is the charge density of a homogeneously charged cylinder with the diameter of the anode and the length of the vessel that produces a potential drop along its axis of 136 V.

Figure 2(c) shows the discharge current in the plasma vessel as a function of the discharge voltage. The slope $\Delta I/\Delta U_{\text{discharge}}$ corresponds to a conductivity of 16 μS. Linear extrapolation indicates for the given Ar gas pressure in the plasma vessel a zero current discharge voltage of 270 V. This demonstrates that this Penning ion source readily produces ions with kinetic energies higher than 400 eV, even with zero discharge potential. Therefore, this kind of ion source does not produce very low energy ions near the *h*-BN penetration threshold only, even if the lowest possible discharge voltages are used. Furthermore, it has to be mentioned that the setup with an electrostatic ion energy analyzer does not allow to discriminate the ion charge state, e.g., singly charged from doubly charged ions, and it is blind to neutrals. Below we show with the help of scanning tunneling microscopy experiments that the ion beam under investigation must also contain neutrals with enough kinetic energy for *h*-BN penetration. In order to decrease the perpendicular momentum component of the ions, the incidence angle may be varied, as it is shown for one example below.

IV. NEUTRAL ATOM IMPLANTATION

The interaction of the ion beam with a single layer of *h*-BN on Rh(111) led to the observation of nanotents, i.e., protrusions with single atom height.[4,11] The nanomesh is a single layer of hexagonal boron nitride on Rh(111). The lattice mismatch and the site selective bonding between the BN and the Rh atoms lead to the formation of a superhoneycomb structure with a unit cell of 13×13 BN units on 12×12 Rh atoms. This forms a "mesh" like structure with pores and wires.[10] In the wire regions, the *h*-BN has no active bonding to the substrate and "floats" above the Rh, while in the 2 nm pores the nitrogen binds on top of the Rh to the substrate. The nanotent interstitial defects have atomic dimensions and selectively occupy the wire-crossing sites of the *h*-BN nanomesh.

Figure 3(a) shows a nanotent as observed after Ar^+ ion irradiation. The tunneling microscopy image and the height profile display the atomic dimension and its location at a nanomesh wire-crossing site. Surprisingly, this nanotent may not be due to a positive ion impact as it was observed before,[4] because the positive ions have been blocked with a

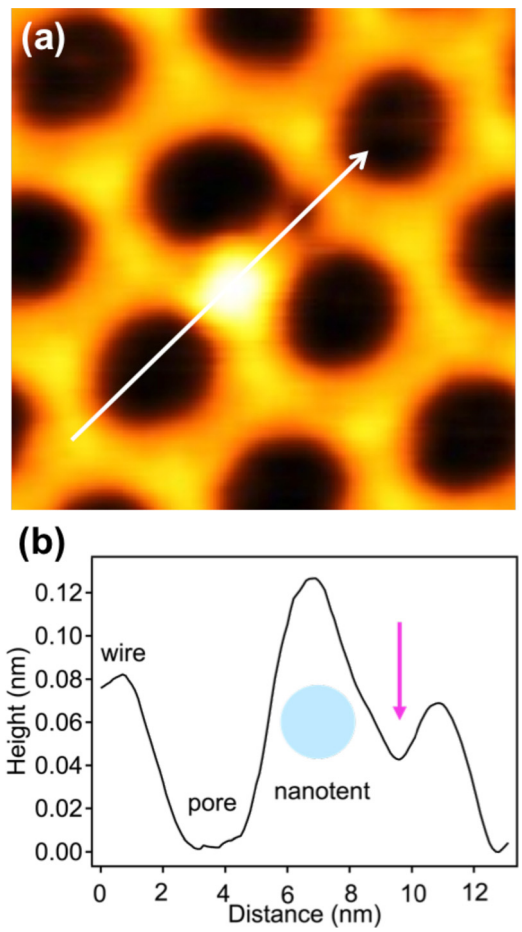

FIG. 3. (Color online) Nanotent formation after Ar^+ ion irradiation (discharge voltage 500 V, sample bias +800 V) and corresponding height line profile. (a) Nanotent (single atomic protrusion) as observed on the *h*-BN nanomesh by STM ($9.5 \times 9.5\,nm^2$, $U_t = -1.20$ V, and $I_t = 0.50$ nA). The protrusions emerge at wire-crossing sites of the *h*-BN nanomesh. (b) The height profile indicates the four structural elements: Nanotent, wire and pore, and the pink arrow indicates a vacancy defect caused by energetic atom impact.

positive bias applied to the sample during irradiation. From the fact that negative argon ions are not stable, we conclude that the ion gun also promotes neutral atoms into a hyperthermal state that allows for the penetration of a single layer of *h*-BN. They are expected not to have a larger kinetic energy than the Ar^+ ions, which may transfer all momentum in a head on collision on a neutral Ar atom at rest. For *h*-BN penetration, the atoms have to knock out a boron or a nitrogen atom and thus have an energy larger than the corresponding B or N displacement energy, which is in the order of 20 eV.[16] For much higher energies they penetrate deeper into the substrate, adatoms may be formed,[3] and eventually, sputtering is expected. In contrast to ions, neutrals do not carry any potential energy as it is, e.g., the first ionization energy (19.8 eV for Ar^+).[17] Our experiments thus confirm that the kinetic energy is the most important component for the formation of vacancy defects in *h*-BN, since we can observe defects created with ions or hypothermal neutrals.

In order to study the energy dependence of the nanotent formation process, we applied different bias voltages to the sample during ion irradiation. Figure 4(a) shows the sample current as a function of the bias voltage with a discharge voltage of 500 V and a discharge current of 1.2 mA for a beam impinging 55° from the normal. The Ar pressure in the chamber is 7×10^{-6} mbar. The sample current versus bias voltage U_b curve reflects the integrated energy spectrum up to the bias voltage. The constant sample current above 500 V indicates an upper energy cut-off, though at a lower energy than the corresponding normal incidence spectrum. This can be rationalized by the deflection of ions with a perpendicular momentum component $p_\perp$ smaller than $\sqrt{2mqU_b}$, where m is the mass of Ar and q is the charge.

The negative sign of the sample current higher than the ion energy threshold ($-0.05\,\mu$A) must be due to electrons that were created by the operation of the ion gun. Due to their low mass and energy, they are however not expected to cause atomic displacements. For further consideration, we subtract this electron current from the sample current in order to estimate the ion current for all positive bias voltages. In Fig. 4(b), we compare the corresponding ion current density and the nanotent density for a 10 s exposure of the sample to the Ar^+ ion beam as a function of bias voltage. Both decrease with increasing bias, and for zero bias, we determine a nanotent yield of about 0.2 protrusions per ion. This yield is lower than that reported in Ref. 4, also because the experiments in Ref. 4 were conducted with a discharge voltage of 780 V. Interestingly, nanotents are also formed for bias voltages exceeding the kinetic energy threshold for ions generated with a discharge voltage of 500 V. The yellow bar in Fig. 4(b) indicates that about one quarter of the zero bias

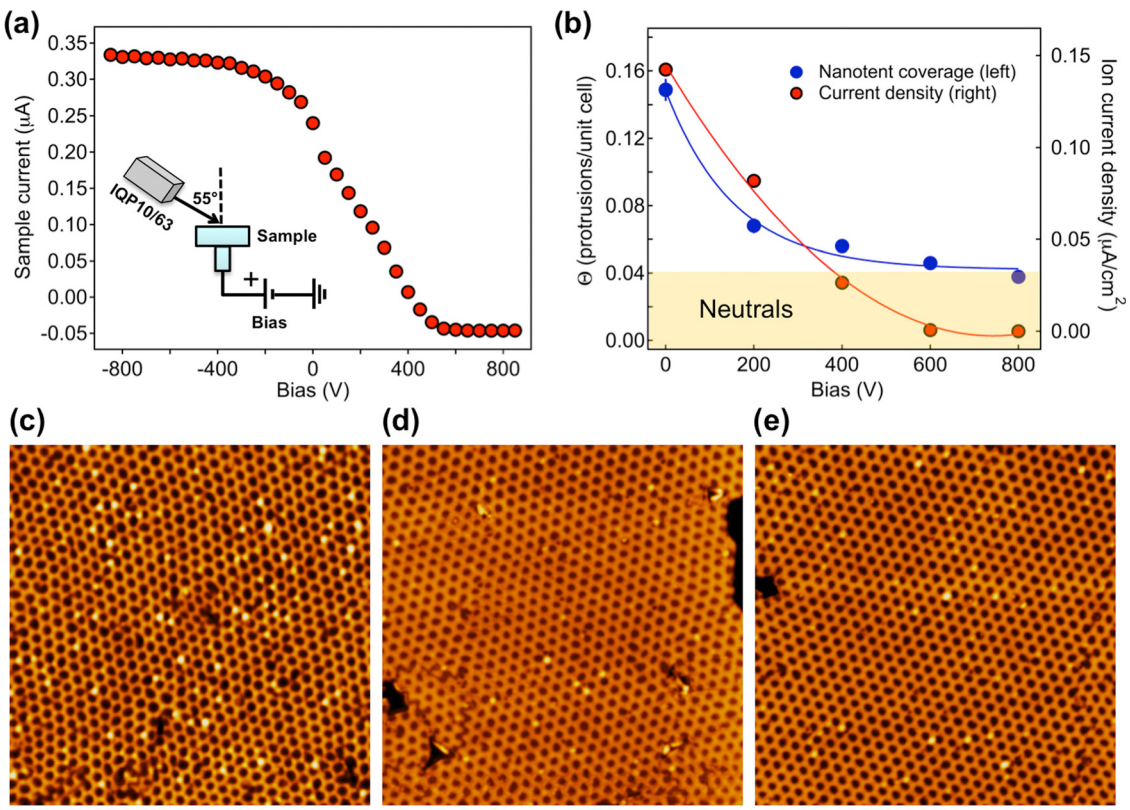

FIG. 4. (Color online) Sample current and Ar nanotent coverage with different applied sample bias and an ion source discharge voltage of 500 V, zero discharge potential, and a discharge current of 1.2 mA. (a) Sample current that changes with different bias voltages. The inset gives the experimental setup with the impinging angle of 55° and the applied bias voltage. (b) Ion current density (red, right) and resulting nanotent coverage (blue, left) for a 10 s exposure. The yellow bar labeled "Neutrals" indicates the portion of nanotents formed by neutral atoms. (c)–(e) Room-temperature STM images ($95 \times 95\,nm^2$, $U_t = -1.20$ V, and $I_t = 0.50$ nA) for different applied positive bias voltages during the precedent implantation process. (c) No positive bias voltage applied. (d) +400 V. (e) +800 V.

nanotents is created by neutrals. This may only be explained by impact of hyperthermal neutral atoms with an energy exceeding the displacement energy of boron or nitrogen.

V. CONCLUSIONS

In conclusion, we report the ion energy spectra of a commercial cold cathode Penning ion source that was used to produce atomic defects on surfaces. Despite the application of a positive bias voltage above the ion energy cut-off, we observe atom impacts with energies higher than the penetration threshold, which indicates hyperthermal neutral atoms in the ion beam of such ion sources.

ACKNOWLEDGMENTS

Financial support from the Swiss National Science Foundation, an UZH Forschungskredit (HYC), and from the EC under the Graphene Flagship (Contract No. CNECT-ICT-604391) is gratefully acknowledged.

[1]C. H. Kim, S. H. Ahn, and D. Y. Jang, Vacuum **86**, 1014 (2012).
[2]H. Niehus, W. Heiland, and E. Taglauer, Surf. Sci. Rep. **17**, 213 (1993).
[3]T. Michely and C. Teichert, Phys. Rev. B **50**, 11156 (1994).
[4]H. Y. Cun, M. Iannuzzi, A. Hemmi, S. Roth, J. Osterwalder, and T. Greber, Nano Lett. **13**, 2098 (2013).
[5]S. Standop, O. Lehtinen, C. Herbig, G. Lewes-Malandrakis, F. Craes, J. Kotakoski, T. Michely, A. Krasheninnikov, and C. Busse, Nano Lett. **13**, 1948 (2013).
[6]E. H. Åhlgren, S. K. Hämäläinen, O. Lehtinen, P. Liljeroth, and J. Kotakoski, Phys. Rev. B **88**, 155419 (2013).
[7]H. Y. Cun, M. Iannuzzi, A. Hemmi, J. Osterwalder, and T. Greber, Surf. Sci. **634**, 95 (2015).
[8]Q. Ma *et al.*, ACS Nano **8**, 4672 (2014).
[9]M. Corso, W. Auwärter, M. Muntwiler, A. Tamai, T. Greber, and J. Osterwalder, Science **303**, 217 (2004).
[10]S. Berner *et al.*, Angew. Chem. Int. Ed. **46**, 5115 (2007).
[11]H. Y. Cun, M. Iannuzzi, A. Hemmi, J. Osterwalder, and T. Greber, ACS Nano **8**, 1014 (2014).
[12]H. Y. Cun, M. Iannuzzi, A. Hemmi, J. Osterwalder, and T. Greber, ACS Nano **8**, 7423 (2014).
[13]Z. Nouri, R. Li, R. A. Holt, and S. D. Rosner, Nucl. Instrum. Methods Phys. Res., Sect. A **614**, 174 (2010).
[14]J. Nagy, Nucl. Instrum. Methods **32**, 229 (1965).
[15]P. Rohwer, H. Baumann, K. Bethge, and W. Schütze, Nucl. Instrum. Methods Phys. Res. **204**, 245 (1982).
[16]J. Kotakoski, C. H. Jin, O. Lehtinen, K. Suenaga, and A. V. Krasheninnikov, Phys. Rev. B **82**, 113404 (2010).
[17]F. Aumayr, S. Facsko, A. S. El-Said, C. Trautmann, and M. Schleberger, J. Phys.: Condens. Matter **23**, 393001 (2011).